Reconstruction of Cortical and Cancellous Bone in Tibia with Osteogenesis Imperfecta

N. Mansor, Y. M. Beh, M. H. Mat Som, K. S. Basaruddin, N. Mustafa, H. Yazid and A. F. Salleh

School of Mechatronic Engineering, Universiti Malaysia Perlis

mhanafi@unimap.edu.my

Abstract—Osteogenesis Imperfecta (OI) is the bone fragility disorder that leads to long bone bowing. Finite Element Analysis (FEA) has become the tool of choice to assess behaviour structural within bones. Currently, the FEA performed on the tibia is based on the bone constructed without considering different components of the bone, where the bone was created as a single material. In an attempt to further investigate the bone with OI, the present study was conducted to investigate the mechanical stress distribution using finite element model of the OI affected tibia. The model was reconstructed from the CT images composed of cortical and cancellous bones obtained from Osirix database. The segmentation of the cortical and cancellous of the tibia was performed on 346 images using two different methods which are global thresholding and the selection of the binary object. The segmented images were used to develop a three-dimensional model of the tibia using VOXELCON software. The boundary conditions were set to the meshed model in preparation for the finite element analysis using the same software. Displacements ranging from 5 mm to 35 mm were assigned to a point in between the proximal and distal of the tibia model. In the coronal plane, the highest stress levels were recorded on the medial side of the cortical bone, whereas in the sagittal plane, the highest stress levels were recorded on the anterior side of the cortical bone when the model was subjected to 35 mm displacement. The cancellous bone, however, showed lower stress levels on both planes when subjected to similar displacement. With each increment of displacement, the model experienced more stress and caused the higher percentage volume of individual cortical and cancellous that exceed critical stress of 115 MPa. There were no significant differences in the percentage volume of voxels affected between the cortical and cancellous bones for both coronal and sagittal planes with the p-value of 0.29 and 0.32 respectively (p > 0.05). There was no significant difference obtained for the percentage volume of voxels affected between the coronal and sagittal planes with the p-value is 0.13 (p > 0.05).

Index Terms—Cortical; Cancellous; Finite Element; Osteogenesis Imperfecta; Stress Distribution; Tibia.

I. INTRODUCTION

Osteogenesis Imperfecta (OI) is the bone fragility disorder occurred in most children with the ratio of 1 in 10000 to 1 in 20000 newborns in the United States [1]. Bone fragility in OI has a characteristic of low bone mass. Individuals with OI tend to have very low bone density and both trabecular and cortical thickness are decreased [2].

Finite element analysis (FEA) has become the tool of choice to assess structural behaviour within bones. Accurate three-dimensional (3D) models of long bones are crucial in the application of FEA. Computed tomography (CT) or Magnetic Resonance Imaging (MRI) images are the main sources of data required to perform 3D model of bones [3].

There were two processes involved in the 3D reconstruction of the tibia, image segmentation and image reconstruction. Image processing techniques were used to remove unnecessary information in the images and to separate the cortical and the cancellous component of the tibia. A 3D model of the tibia composed of individual cortical and cancellous component was made available via the VOXELCON; a software specialised in generating 3D models from a set of images. Next, this model was set to mimic the OI affected tibia by using the OI bone parameter found in the literature. Finally, the model underwent finite element analysis to study the stress distribution in individual cortical and cancellous of the tibia with OI.

Global thresholding method is an image processing technique widely used in medical image segmentation [4, 5]. This method searches the boundaries between regions based on discontinuities in intensity levels. Thus, this method can be used to obtain the specific region of interest, i.e. cortical and cancellous bone, while ignoring the remainder of the image. The accuracy of separation between cortical and cancellous bone could be enhanced by combining the global thresholding method with other image processing techniques such as edge enhancement, region growing and also by considering the pixel intensity of local neighbourhood of the image [6]. Automatic segmentation of cortical and cancellous components was developed by using an algorithm to identify the cortical and cancellous volumes [7]. The entire bone region was extracted first, followed by extraction of the cortical region. The cancellous region can be obtained by subtracting the cortical region from the entire bone region. Semi-automated segmentation using algorithms based on energy minimising, spline curves, and deformable model methods have been proposed by Gelaude et al. [8] in the segmentation of cortical and cancellous components.

Caouette et al. [1] developed the tibia models to biomechanically predict the risk of tibial fracture in patients with OI. The fracture risk of these models was examined via principal strain criteria through the modelling of two-legged hopping loading which was lateral and torsional loading. Material properties were assumed to be isotropic where the elastic modulus of cortical bone varying from 5 to 19 GPa and a Poisson's ratio of 0.3 obtained from nano indentation test conducted on the paediatric OI bone [9-11]. Previous studies conducted by Fritz et al. [12] and Albert et al. [13] found the yield stress lying between 110 and 115 MPa.

The objective of this study was to develop a patient-specific finite element model of the tibia that mimics the OI bone using available CT images. This patient-specific model was used to analyse the mechanical stress distribution and the total number of voxels affected for individual cortical and cancellous due to displacement applied to the model in finite

element analysis. It was hypothesised that the cortical bone was prone to greater stress compared to the cancellous bone based on their mechanical properties.

II. METHODOLOGY

The study was divided into three parts, image segmentation, 3D tibia model, and finite element analysis. Standard tibia bone was acquired from CT images in Osirix database [14]. The CT image of the lower limb was composed of 346 slices of images in DICOM format. It contains information such as two bones (tibia and fibula) and soft tissues. In this study, only the left tibia from the CT image was processed for the generation of the 3D model. As shown in Figure 1, the pixel intensity for the soft tissues mostly in the grey levels whereas there are some white levels distributed in the images indicating the outer region of the bone. However, the intensity of the inner regions of the bone was quite similar with the intensity of the soft tissues.

A. Image Segmentation

In the image segmentation part, MATLAB was primarily used to process the CT images. Generally, global thresholding method was adopted to separate between the bone and soft tissues. This method is used to separate the entire bone region from the soft tissues as determined from the pixel grayscale values. A specific threshold, T was defined in this binarisation technique, where based on the grey levels, each pixel of the CT image was classified into bone (foreground) and soft tissue (background). For a pixel of intensity, $I(x,y)$,

$$I(x, y) = \begin{cases} 1 & \text{if } I(x, y) > T \\ 0 & \text{if } I(x, y) < T \end{cases} \tag{1}$$

Further processes were required to obtain a clean image of the cortical and cancellous bone. Most of the processing techniques employed are an available function in the MATLAB.
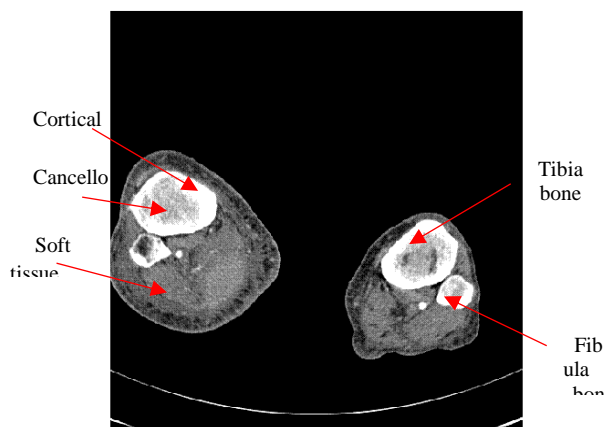

Figure 1: Original CT image acquired from OSIRIX database [14]

B. 3D Tibia Model

A patient-specific 3D model of tibial bone was generated using VOXELCON (2014) from two sets of images; 346 images of the segmented cortical component and 295 images of the segmented cancellous component. For simplicity, the 3D model was only generated for left tibia for further analysis.

The material properties for each cortical and cancellous were defined based on previous studies. The tibia was assumed to be isotropic with Young's modulus for the cortical bone was set to 15 GPa while Young's modulus for the cancellous was set to 10 GPa [9]-[11]. Poisson's ratios for both cortical and cancellous bones were set to 0.3 [10].

C. Finite Element Analysis

To introduce the bowing as in the OI bone, seven cases of displacements were simulated in VOXELCON. For all displacement cases, the voxel model was fully constrained in all directions where the displacement and rotation were fixed at the proximal (upper end) and distal (lower end) tibia to prevent rigid body motion. The middle part of the tibial shaft was applied with displacement in posteroanterior direction for the coronal plane and lateral direction for the sagittal plane as illustrated in Figure 2. Seven displacements were applied to the surface of the middle parts of the tibial shaft for both coronal and sagittal plane cases. For the first simulation, the displacement, d of 5 mm was applied to the model in posteroanterior direction for the coronal plane and in the lateral direction for the sagittal plane. The displacements were increased by 5 mm for the next six simulations. The model was analysed based on the fracture strength which was assumed to be approximately 115 MPa [13].

III. RESULTS AND DISCUSSIONS

A. Image Segmentation

Figure 3 shows the sample slices of segmented cortical and cancellous bone. By using the global thresholding method, the bone was successfully distinguished from the soft tissues as shown in Figure 3(a). Next, the fibulas for both legs were removed that resulted in the image as shown in Figure 3(b). At this stage, the cortical bone has been successfully extracted from the image. Finally, the cancellous bone was extracted by selecting the binary object of the cancellous bone.
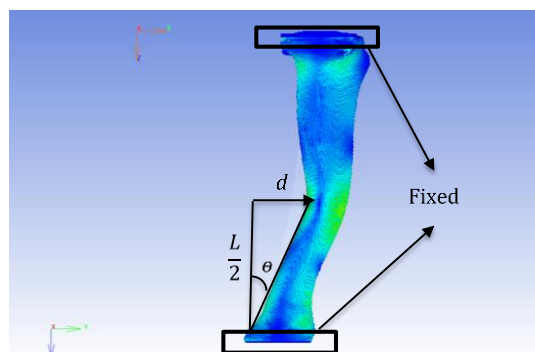

Figure 2: The displacement point, d and boundary conditions for analysis. The displacement was applied in a posteroanterior direction for the coronal plane and in the lateral direction for the sagittal plane.
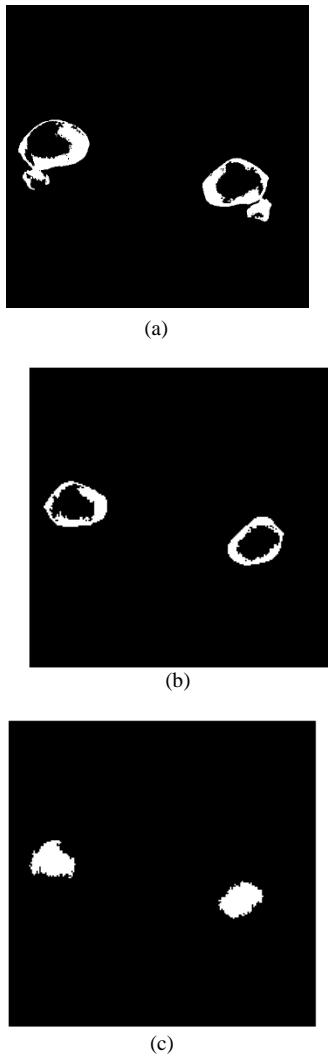
(a)

(b)

(c)

Figure 3: Segmented image for (a) tibia and fibula bones (b) cortical (c) cancellous

One of the goals of this study was to differentiate the cortical and cancellous bone using image processing techniques. The segmentation of bone tissue from CT images was a complex and challenging procedure due to the cortical and cancellous structures. Cortical tissue which is the outer part of the bone is very dense compared to the cancellous tissue which is the inner part of the bone has a less intensity in CT images. Also, the intensity value for the same tissue varied between slices. Due to high-intensity values in the cortical bone, the approach of the global thresholding-based method was implemented to segment the cortical. The same approach has been implemented by Zhang et al. [4]. The current study shows that the global thresholding able to separate the bone tissue from the remainder of the images.

B. 3D Tibia Model

Figure 4 shows the 3D model of tibia generated using VOXELCON software. This tibia model bone was reconstructed from 346 images of cortical components and 295 images of cancellous components. The tibia voxel model generated consists of 65,2515 voxel elements of 168 mm length of cortical bone and 19,2082 voxel elements of 147 mm length of the cancellous bone. The current study was only able to extract the cancellous component from 295 images due to poor image quality. The images, especially in proximal and distal of the tibia, show poor contrast between

the cortical and cancellous components. Thus, it was not possible to separate the two components accurately. Hence, the proximal and distal of the cancellous bone were left out in the generation of the tibia model. However, the effect of these components was assumed to be minimal since fixed constrain were applied to the proximal and distal of the tibia.
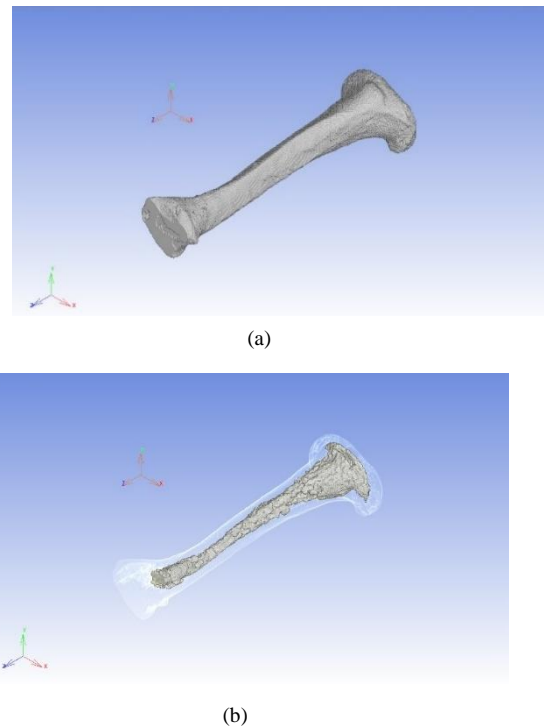

(a)

(b)

Figure 4: Three-dimensional voxel model of tibia generated using VOXELCON software (a) cortical component (b) cancellous component

C. Finite Element Analysis

Table 1 shows that the maximum von Mises stress increases with each increment of displacement. When the tibia was subjected to displacements from 5 to 35 mm in the coronal plane, the von Mises stress increased from 5 GPa to the maximum of 37 GPa. Whereas, in the sagittal plane, the von Mises stress was at 9 GPa when the tibia was applied with a displacement of 5 mm and increased to 66 GPa with a displacement of 35 mm.

The tibia model was analysed using the fracture strength which was assumed to be approximately 115 MPa, based on the nano indentation data of the previous literature [10, 11]. Figure 5 shows the critical areas of the bone where the stress level recorded were beyond 115 MPa due to 35 mm displacement. In Figure 5(a), the areas of highest stress were observed in the anterior of the cortical bone with severe anterior bowing. In comparison, the areas of highest stress in the sagittal plane as shown in Figure 5(b) were significant on the medial side of the cortical bone with severe medial bowing. The areas with the highest stress on the cancellous bone was less affected in both coronal and sagittal planes.

The voxel and volume of tibia recorded beyond the fracture strength were affected by the magnitude of the displacement applied to the bone. A total number of voxels affected and the percentage volume in the tibia bone consist of cortical and cancellous on coronal and sagittal planes are illustrated in Figure 5 and 6. For both coronal and sagittal planes, the contours showed that the highly affected voxels on both cortical and cancellous bone occurred for the severe

deformity due to 35 mm displacement. The plot demonstrates that the percentage volume of voxels affected was quite similar for the displacements of 5 mm, 25 mm, 30 mm and 35 mm in both planes. Whereas, the percentage volume was much higher in the coronal plane for the displacements of 10 mm, 15 mm and 20 mm.

The result of the t-test shows that there were no significant differences in the percentage volume of the voxels affected between the cortical and cancellous bones in both coronal and sagittal planes where the p-value are 0.29 and 0.32 respectively ($p < 0.05$). The result also shows that there were no significant differences in the total percentage volume of voxels affected between the coronal and sagittal planes with the p-value is 0.13 ($p > 0.05$).

Table 1
The Maximum Von Mises Stress due to Displacements Constrain Applied on The Middle Tibia Shaft on the Coronal and Sagittal Plane.

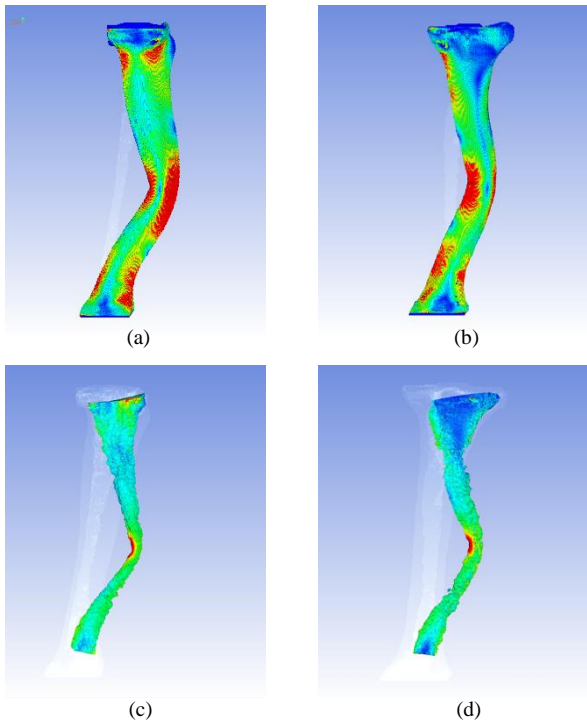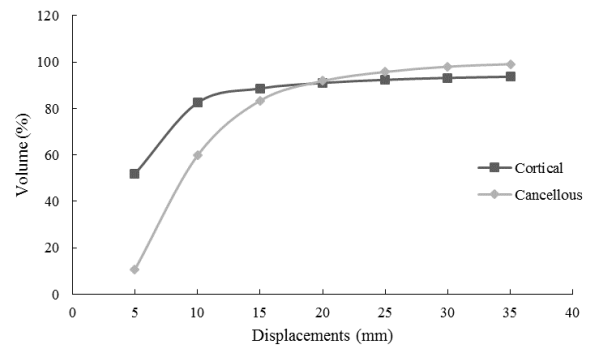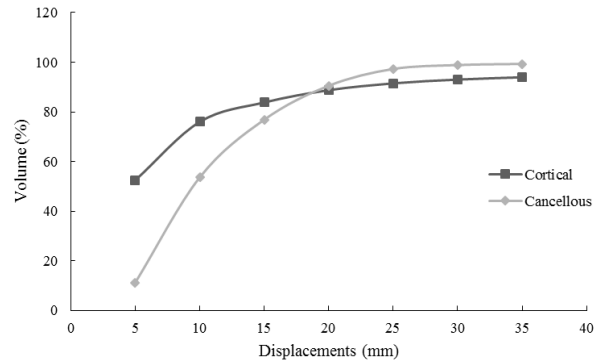| Displacements (mm)	Maximum von Mises Stress (GPa)	
	Coronal	Sagittal
5	5.31	9.49
10	10.62	18.97
15	15.94	28.46
20	21.25	37.95
25	26.56	47.44
30	31.87	56.92
35	37.18	66.41

Figure 5: Stress distribution on the tibia due to 35 mm displacement constrain. (a) Cortical bone on coronal plane (b) Cortical bone on sagittal plane (c) Cancellous bone on coronal plane (d) Cancellous bone on sagittal plane

Figure 6: Percentage volume of voxels recorded beyond fracture strength of 115 MPa in cortical and cancellous bones due to various displacement constrains applied to the bone in (a) coronal plane (b) sagittal plane.
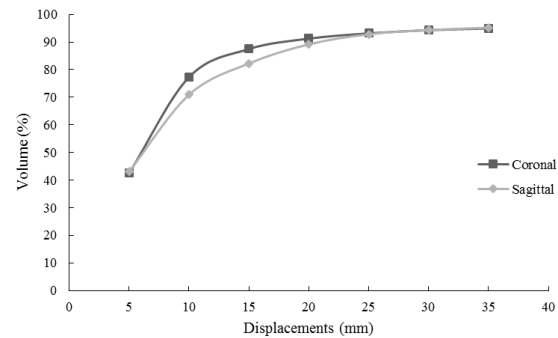

Figure 7: The percentage volume of total voxels of cortical and cancellous bones beyond fracture strength due to various displacement constrains applied to the bone in the coronal and sagittal plane. The fracture strength for was set to 115 MPa.

This study demonstrated the feasibility of using segmented cortical and cancellous from available CT scan imaging to create the bone geometry of the OI tibia. The key parameters in creating the FE model included tibia geometry, material properties and boundary conditions. Young's modulus for the model is taken from nano indentation tests conducted on type III and type IV OI bone specimens [11]. The tests were used to characterise the material properties of bone tissue with OI. Compared to normal bone tissue, the OI bone exhibit more isotropic material properties due to abnormal collagen network. Both cortical and cancellous have lower Young's modulus compared to normal bone. However, the relative decrease in modulus of cortical bone exceeds the cancellous bone. OI appears to affect the cortical bone properties compared to cancellous due to the higher collagen density in cortical.

The purpose of the present study was to investigate the stress distribution in cortical and cancellous of the OI tibia from the finite element analysis model to study the influence of OI deformity. The von Mises stress distribution shows that the stress levels increased with the higher level of displacements applied. The deformity or bowing also increase with the levels of displacements. This happens to both cortical and cancellous bone. In comparison, the finite element model developed by Fritz et al. [15] show the maximum von Mises stress distribution values increase with the level of bowing. Fan et al. [16] concluded that the stress distribution deteriorates by deformity where the deterioration increased with increase in severity.

The von Mises stress was also used to examine the locations of fracture initiation which referred to the highest stress levels. According to the literature, Fritz et al. [12] describe the contour map of maximum von Mises stress to highlight the areas correlated with the fracture risk. The current model with the highest displacement of 35 mm shows more areas of red contour. It was found that there was a significant difference in the areas of highest stress levels between the cortical and cancellous bone. The cortical bone experiences higher stress levels compared to the cancellous bone.

IV. CONCLUSION

This study employs clinically available images of CT images of the standard tibia. Results from the image processing highlighted the importance of bone geometry reconstruction for further analysis. It allowed 3D reconstruction of the tibia from the segmented cortical and cancellous images. Then, the mechanical stress distribution of tibia affected with OI was successfully investigated using static stress analysis. In the finite element method, the static stress analysis did not account for the effect of muscle and tendon connected to the bone.

ACKNOWLEDGEMENT

REFERENCES

[1] C. Caouette et al., "Biomechanical analysis of fracture risk associated with tibia deformity in children with osteogenesis imperfecta: a finite element analysis," *J. Musculoskelet. Neuronal Interact,* vol. 14, no. 2, pp. 205–12, 2014.

[2] C. Caouette, N. Ikin, I. Villemure, P. J. Arnoux, F. Rauch, and C. É. Aubin, "Geometry reconstruction method for patient-specific finite element models for the assessment of tibia fracture risk in osteogenesis imperfecta," *Med. Biol. Eng. Comput.*, pp. 1–12, 2016.

[3] K. Rathnayaka, T. Sahama, M. A. Schuetz, and B. Schmutz, "Effects of CT image segmentation methods on the accuracy of long bone 3D reconstructions," *Med. Eng. Phys.*, vol. 33, no. 2, pp. 226–233, 2011.

[4] Y. Zhang, Z. He, S. Fan, K. He, and C. Li, "Automatic Thresholding of micro-CT trabecular bone images," in *Proceedings of the 1st International Conference on BioMedical Engineering and Informatics*, Sanya, China, 2008, vol. 2, pp. 23–27.

[5] D. L. Pham, C. Xu, and J. L. Prince, "Current methods in medical image segmentation," *Annu. Rev. Biomed. Eng.,* vol. 2, no. 1, pp. 315-337, 2000.

[6] E. Cendre, V. Kaftandjian, G. Peix, M. Jourlin, and D. Babot, "An investigation of segmentation methods and texture analysis applied to tomographic images of human vertebral cancellous bone," *J. Microsc.*, vol. 197, no. 3, pp. 305–316, 2000.

[7] G. Rizzo, D. Tresoldi, E. Scalco, M. Mendez, A. M. Bianchi, and A. Rubinacci, "Automatic Segmentation of Cortical and Trabecular Components of Bone Specimens Acquired by pQCT," in *30th Annual International Conference of the IEEE EMBS*, Vancouver, Canada, 2008, pp. 486–489.

[8] F. Gelaude, J. Vander Sloten, and B. Lauwers, "Semi-automated segmentation and visualisation of outer bone cortex from medical images," *Comput. Methods Biomech. Biomed. Engin.*, vol. 9, no. 1, pp. 65–77, 2006.

[9] Z. Fan, P. Smith, E.C. Eckstein and G.F. Harris, "Mechanical properties of OI Type III human bone tissue measured by nano indentation," *J. Biomed. Mater. Res.*, vol. 79A, pp. 71–77, 2006.

[10] Z. F. Fan, P. Smith, F. Rauch, and G. F. Harris, "Nano indentation as a means for distinguishing clinical type of osteogenesis imperfecta," *Compos. Part B Eng.*, vol. 38, no. 3, pp. 411–415, 2007.

[11] Z. Fan, P. a Smith, G. F. Harris, and F. Rauch, "Comparison of Nano indentation Measurements between Osteogenesis Imperfecta Type III and Type IV and Between Different Anatomic Locations (Femur / Tibia versus Iliac Crest)," *Connect. Tissue Res.*, vol. 48, pp. 70–75, 2007.

[12] J. M. Fritz, Y. Guan, M. Wang, P. A. Smith, and G. F. Harris, "A fracture risk assessment model of the femur in children with osteogenesis imperfecta (OI) during gait," *Med. Eng. Phys.*, vol. 31, pp. 1043–1048, 2009.

[13] C. Albert, J. Jameson, P. Smith, and G. Harris, "Reduced diaphyseal strength associated with high intracortical vascular porosity within long bones of children with osteogenesis imperfecta," *Bone*, vol. 66, pp. 121–130, 2014.

[14] "OsiriX | DICOM Image Library." [Online]. Available: http://www.osirix-viewer.com/resources/dicom-image-library/. [Accessed: 15-May-2017].

[15] J. Fritz, N. Grosland, P. Smith, and G. Harris, "Improved mesh for a finite element model of fracture risk assessment in Oseogenesis Imperfecta," *35th Annual Conference of the American Society of Biomechanics*, Long Beach, 2011.

[16] Z. Fan, P. Smith, K. Reiners, and S. Hassani, "Biomechanics of Femoral Deformity in Osteogenesis Imperfecta (OI): A Quantitative Approach to Rehabilitation," in *Proceedings of the 26th Annual International Conference of the IEEE EMBS*, San Francisco, 2004, pp. 4884–4887.